Exploring 2D Subsurface Structures: Analyzing Electromagnetic Data in the Frequency Domain with Two Distinct 1D Inversion Techniques

Sabrina Ashik

The University of British Columbia

ESOC 454/556B

April 26, 2023

1. Introduction

Understanding the structures hidden beneath the Earth's surface is crucial for various applications in geophysics, ranging from resource exploration to environmental monitoring. This project investigates 2D subsurface structures using frequency domain electromagnetic data and various inversion techniques. The goal of this project is to assess the accuracy of 1D inversion methods in recovering 2D subsurface features.

The simulation and inversion processes are facilitated by SimPEG, an open source framework for simulation and gradient based parameter estimation in geophysical applications. Synthetic data and forward simulation is generated using a 1D layered earth model, which is defined by the set of layer thicknesses and the physical properties for each layer. Subsequently, two distinct inversion methods — weighted least squares and iteratively weighted least squares — are employed to recover a 1D model from the generated data, thereby demonstrating the capability to characterize subsurface properties in a 1D context.

By collecting 1D data at various points within the survey region, this project aims to capture the characteristics of 2D subsurface structures and recover a full 2D profile of the structure. This transition from 1D to 2D characterization allows for a more comprehensive understanding of subsurface features.

2. Experimental Setup

The focus of this project is to investigate 2D subsurface structures, particularly relevant for examining sediments beneath basalt formations. Typically, these sediment structures are represented in 2D models to illustrate multiple layers, suggesting their widespread occurrence across large geographic areas. As a result, focusing on inverting the 2D-vertical profile of the structure, rather than addressing it in three dimensions, enables us to simplify the problem without sacrificing any essential information.

Synthetic data will be generated from a reference model drawn from an existing literature (De Groot‐Hedlin & Constable (2004, p. 81)), shown in Figure 1. This reference model illustrates the characteristic features of sedimentary compositions beneath basalt, consisting of a conductive wedge under a high-resistive surface layer atop an intermediate-resistivity basement.

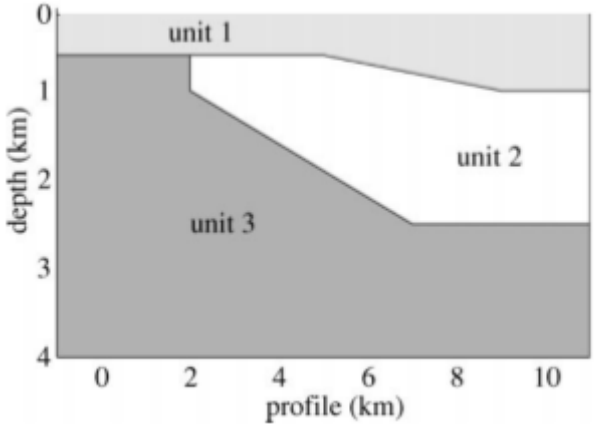

Unit	Resistivity (Ωm)
1	1000
2	10
3	100

Figure 1: Reference model employed for this project

This experimental framework enables a targeted investigation into the strengths and weaknesses of inversion methodologies in capturing large 2D geological formations through straightforward 1D inversion techniques.

3. Physical Property: Electrical Resistivity

The physical property of interest for this project is electrical resistivity (ρ). Electrical resistivity is a crucial physical property that quantifies the materials resist the flow of electric current when subjected to an applied electric field. It serves as a fundamental parameter in geophysical investigations, providing insights into subsurface properties and geological structures.

The relationship between electrical resistivity, electric field (E), and electrical current density (J) is fundamental to understanding the behavior of materials under an electric field. This relationship is expressed as $E = \rho J$, where ρ represents the electrical resistivity of the material.

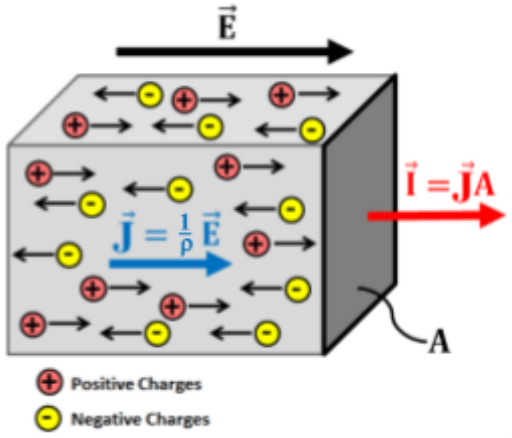

Figure 2: Illustration of Current Density, Electric Field and Resistivity

When an electric field is applied to a material, free charges within the material experience an electrical force, causing them to move through the material, thus constituting an electrical current. The ease with which these charges move through the material determines its electrical resistivity.

The project relies on using electromagnetic systems which operate by inducing electric currents in the ground. These systems follow rules described by Maxwell's equations, which governs how electric and magnetic fields interact and move around. This project examines how the underground's electrical resistivity influences its response to electromagnetic systems. By collecting and analyzing data from these systems, we aim to infer the conductivity layers beneath the surface

4. Survey/Data Collection Method

The survey methodology selected for this project involved a two-coil system with a vertical magnetic dipole source positioned 30 meters above the surface. The receiver was configured to measure the vertical component of the secondary field at a 10-meter offset from the source.

4.1. System Configuration

In the frequency domain electromagnetic (FDEM) system, the transmitter utilizes a wire loop connected to a generator capable of producing a regulated sinusoidal current across various frequencies. This loop is approximated as a magnetic dipole, with the coil typically consisting of multiple turns to enhance effective area.

The receiver, similar to the transmitter, comprises a loop connected to electronics capable of measuring the electromotive force (EMF) induced by external time-varying magnetic fields. Each transmitter loop at a specific frequency corresponds to a receiver loop horizontally offset by a few meters, designed to capture signals at that particular frequency.

Multi-frequency operation is employed in the FDEM system to attain depth resolution, as electromagnetic waves at different frequencies penetrate the Earth to varying depths.

The measured EMF at the receiver is proportional to the rate of change of the magnetic flux through the loop's enclosed area. This flux is estimated as the product of the magnetic flux intensity and the receiver loop's effective area. Subsequently, the measured EMF is utilized to compute the magnetic field (H) at the receiver, given the known frequency, magnetic permeability, and effective area.

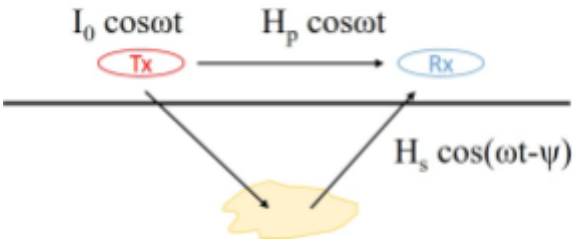

Figure 3: Illustration of the Transmitter and Receiver coils

4.2. Collected data

In FDEM surveys, time-harmonic signals are typically represented as the product of an amplitude factor and an oscillating sinusoidal function. The transmitter current is denoted as $I_0 \cos(\omega t)$, where I_0 represents the peak current and ω denotes the fixed angular frequency.

According to Biot-Savart's law, the primary magnetic field generated by this current follows the form $H_p \cos(\omega t)$, where H_p can be determined based on the distance from the transmitter to any observation point in the whole-space.

Importantly, the primary field is entirely in-phase with the transmitter current. Subsequently, the primary field induces eddy currents in the subsurface, leading to a secondary magnetic field. In most scenarios, this induced current exhibits a phase lag ϕ with respect to the

primary field. Consequently, the secondary magnetic field due to induction takes the form $H_s \cos(\omega t - \phi)$, where H_s is determined by the distance and geometric coupling.

In practice, FDEM systems measure only the secondary field. The convention in FDEM is to use the primary field as the reference to describe the secondary field data. The secondary field can be expressed as a linear combination of two orthogonal sinusoidal signals:

$$H_s \cos(\omega t - \phi) = H_s \cos(\phi) \cos(\omega t) + H_s \sin(\phi) \sin(\omega t)$$

Here, $\cos(\omega t)$ represents a signal in-phase with the source, while $\sin(\omega t)$ represents a signal out of phase with the source. The first term is referred to as the "real" component, while the second term is termed the "imaginary" component.

5. Forward Simulation

5.1. Mesh Generation

To generate a 3D model, first a 2D grid representing the survey region was generated, including some additional padding on the left, right, and bottom edges. This 2D grid, representing the vertical profile of the region, was then projected onto a 3D mesh. Since the structure was assumed to extend significantly along the y-axis, the mesh was designed with only one cell in that direction, as depicted in Figure 4. This simplification is appropriate since it allows us to focus primarily on the 2D profile while still capturing the structure's overall extension.

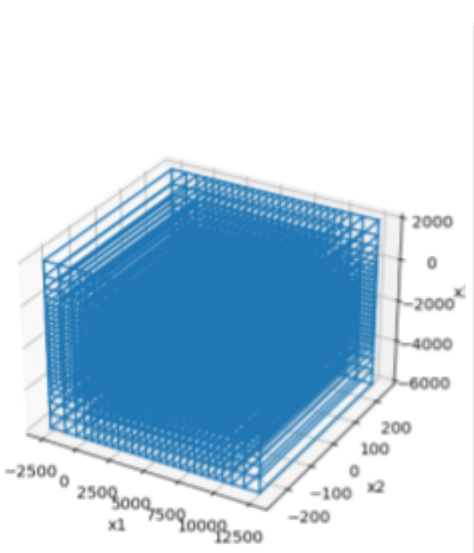

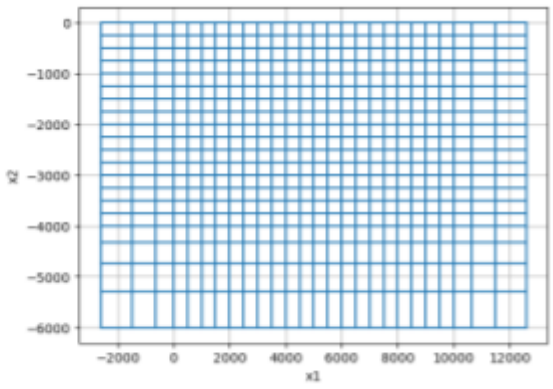

TensorMesh 624 cells

		MESH EXTENT		CELL WIDTH		FACTOR
dir	nC	min	max	min	max	max
x	26	-2,593.50	12,593.50	500.00	1,098.50	1.30
y	1	-250.00	250.00	500.00	500.00	1.00
z	24	-6,010.77	2,010.78	250.00	714.03	1.30

Figure 4: 2D grid and 3D mesh used for modeling

The survey region was discretized into cells measuring 500 meters horizontally and 250 meters vertically. This discretization strategy allowed for the creation of a model with the desired shape while ensuring that the computational load remained manageable by avoiding an excessive number of cells.

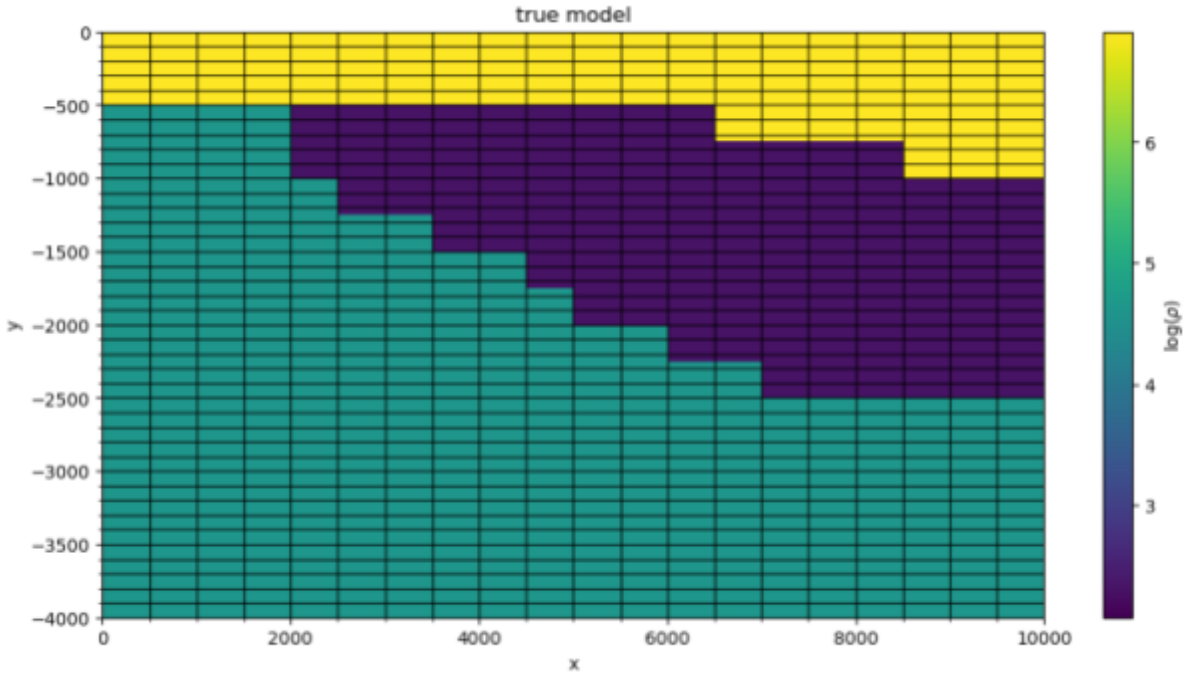

Figure 5: Discretized Reference Model on 2D Mesh with Log Resistivity Values

5.2 Data Collection Method

To capture the entire subsurface structures, 1D data were collected at various points along the 2D grid. The survey methodology described in the preceding section was deployed at intervals of 500 meters across the survey region. A total of 21 evenly spaced soundings were collected, ensuring comprehensive coverage of the survey area.

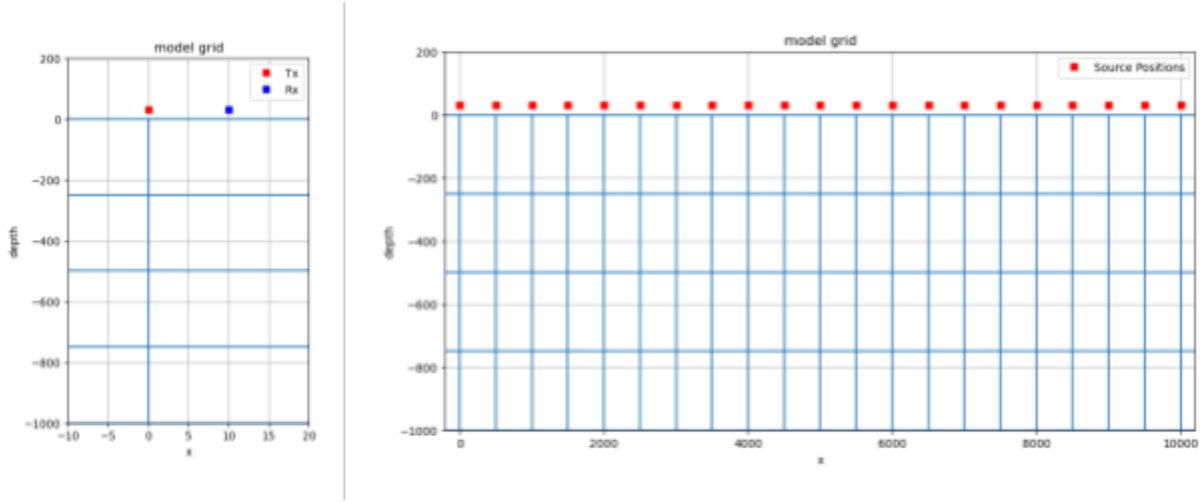

Figure 6: Illustration of the Survey Locations

After the data was collected, Gaussian noise equivalent to 5% was added to better simulate real-world field conditions.

5.3 Approach and Methodology

For each sounding location, a 1D forward simulation was conducted using the Simulation1DLayered class in SimPEG. This simulation class is specifically designed to simulate the FDEM response over a 1D layered Earth for a single sounding.

A 1D layered Earth model is defined by a set of layer thicknesses and corresponding physical properties for each layer, represented here by the logarithmic of the resistivity values. To derive the 1D layered Earth model from the 3D structure, the resistivity and layer thickness values were extracted from the 3D model at the specified sounding locations.

5.4. Frequency Selection

The forward simulations were performed across a range of frequencies to capture the variation in electromagnetic response at different depths. A total of 15 frequencies were sampled, ranging from orders of magnitude of 10e-1 to 10e4. These frequencies were selected to achieve skin depths ranging from 50 m to 16 kilometers, ensuring comprehensive coverage of subsurface structures at various depths. Skin depth, d, the depth at which the EM signal attenuates to 1/e or approximately a third, which can be found by:

$$d \approx 500\sqrt{\frac{1}{\sigma f}} = 500\sqrt{\frac{\rho}{f}}$$

By conducting forward simulations at multiple frequencies and sounding locations, synthetic data were generated to facilitate subsequent inversion and characterization of the 2D subsurface structures within the survey region.

5.5. Testing

To start off, forward simulations were conducted at the far left and far right boundaries of the reference model. This allowed examination of the electromagnetic response of the subsurface at each boundary point. The 1D model and the collected data are illustrated in Figure 7.

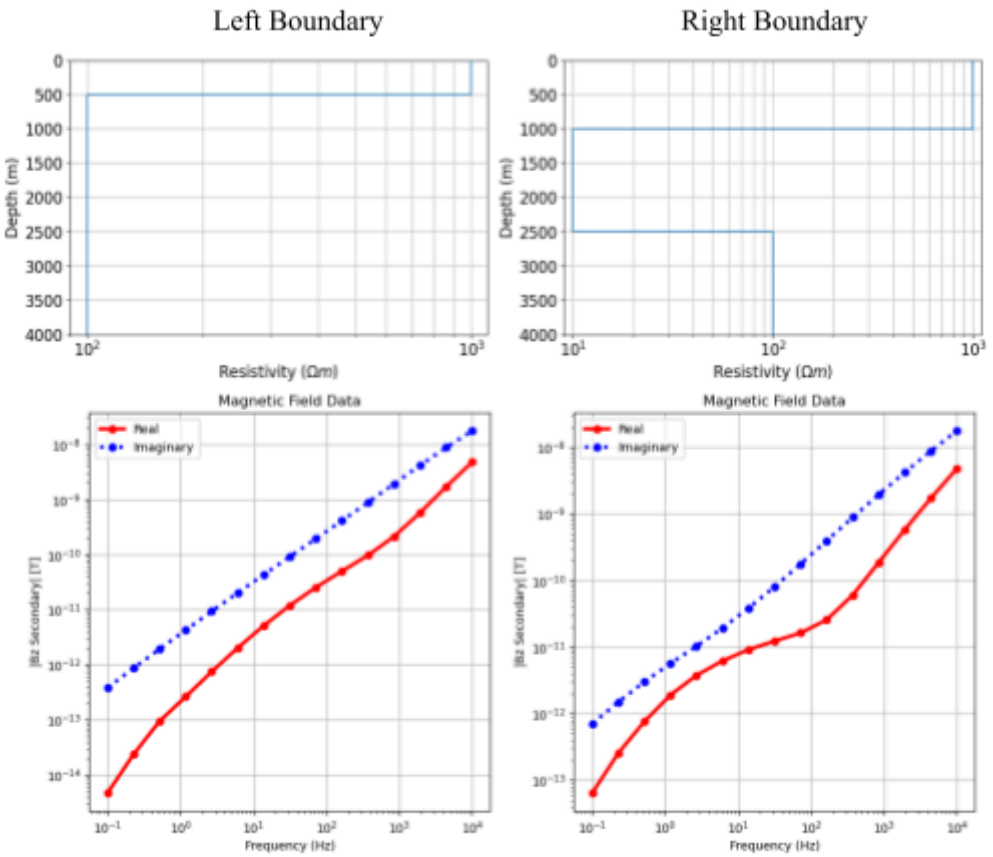

Figure 7: 1D model and Data at the Left and Right Boundaries

6. Inversion Method 1: Weighted Least- Square Method

The first inversion method explored in this project is the weighted least squares approach. This technique is employed to estimate the parameters of a mathematical model by minimizing the sum of the squares of the differences between observed and predicted values. Each data point is weighted based on its estimated uncertainty, with more reliable data points receiving higher weights. By incorporating these weights, the method aims to improve the overall fit of the model to the observed data and provide more accurate parameter estimates. In this project, the estimated uncertainty is set at 5%, consistent with the level of Gaussian noise added to the collected data.

The 1D layered Earth model used for inversion is constructed by defining a large number of layers with exponentially increasing thicknesses. The minimum and maximum depths for inversion are determined based on the estimated resistivity of the deepest layer, ensuring that the layers extend to a multiple of the maximum skin depth. Here, a minimum depth of 50 meters and a maximum depth of 5000 meters were chosen, with the geometric factor adjusted to optimize the solution.

Additionally, a starting model is provided to the inversion process, consisting of an array of estimated resistivity values. This initial estimate helps to start off the inversion process. The same model was also used as the reference model.

The optimization problem is solved using the InexactGaussNewton class, which utilizes the inexact Gauss Newton method with a conjugate gradient solver. This approach enables efficient convergence towards the optimal solution.

Furthermore, several inversion directives were applied to enhance the inversion process:

- UpdatePreconditioner: Jacobi preconditioner is applied to reduce the number of conjugate gradient iterations, with the update frequency set based on model dependency.
- BetaEstimate_ByEig: Starting trade-off parameter (beta) is computed and set based on the largest eigenvalues of the system matrix.
- BetaSchedule: Trade-off parameter is gradually reduced during inversion iterations, ensuring convergence towards the optimal solution.
- TargetMisfit: Inversion terminates when the data misfit equals the target misfit, when the termination criterion is set to achieve a chifact value of 1.

For this method, the cooling factor was set to 2.0, the cooling rate was set to 3, and the chifact was set to 1. However, in order to achieve an optimal recovered model, **the geometric factor** and **BetaEstimate_ByEig** had to be carefully adjusted, as these two parameters had the largest impact on the inversion results.

6.1. 1D Inversion Results

Firstly, the 1D soundings at both the left and right boundaries were inverted to test and refine the inversion parameters. Testing at both boundaries was crucial to the tuning process. This is because the left boundary, characterized by two layers, facilitated assessment under simpler conditions, while the right boundary, with three layers, ensured the robustness of the selected inversion parameters against a more complex model. This comprehensive approach provided valuable insights and validation for the subsequent inversion of the entire survey region.

6.1.1 Tuning the Geometric Factor (GF)

First, the geometric factor was fine-tuned to optimize the inversion process. This parameter directly influences the number of model parameters, as it determines the number of layers between the minimum and maximum depth. A careful balance is required for this parameter, as setting the geometric factor too large may result in excessively large layers, leading to a loss of critical information. Conversely, setting it too small may result in an excessive number of model parameters, imposing a heavy computational burden and potentially yielding an overfitted model. Finding the appropriate geometric factor is crucial for achieving a well-balanced inversion outcome. Following are inversion results of various geometric factors.

GF=1:

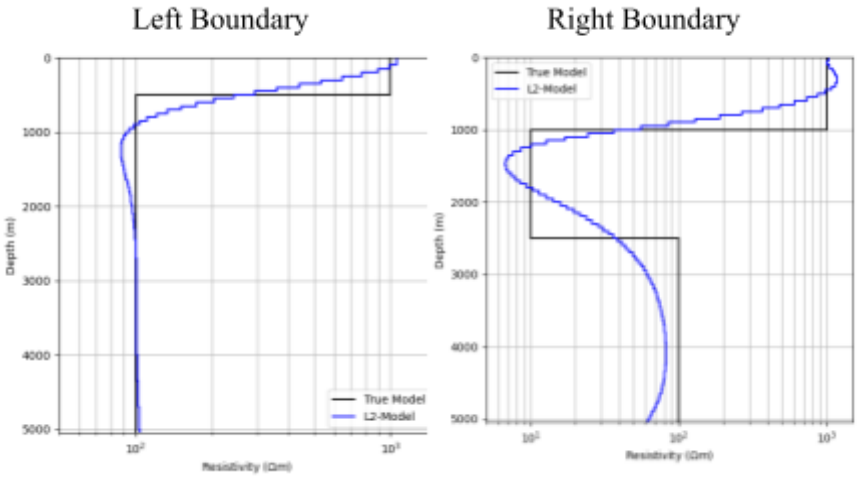

Figure 8: Recovered 1D at the Left and Right Boundaries with GF=1

GF=1.2 (Optimal):

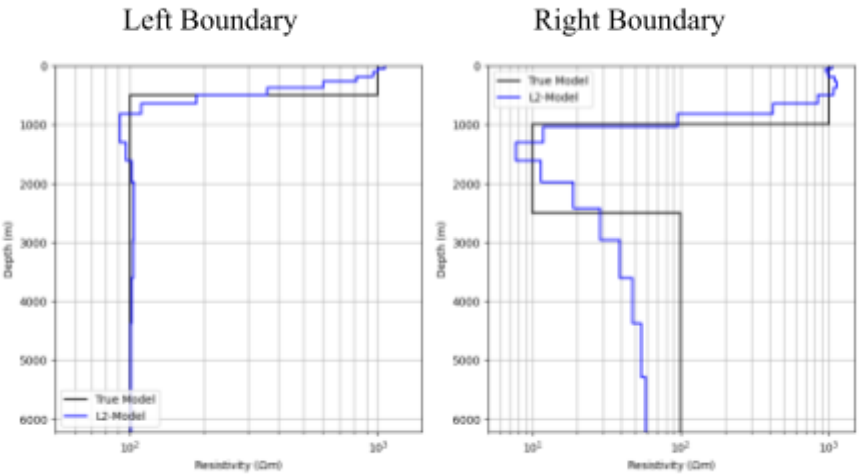

Figure 9: Recovered 1D at the Left and Right Boundaries with GF=1.2

GF=1.5:

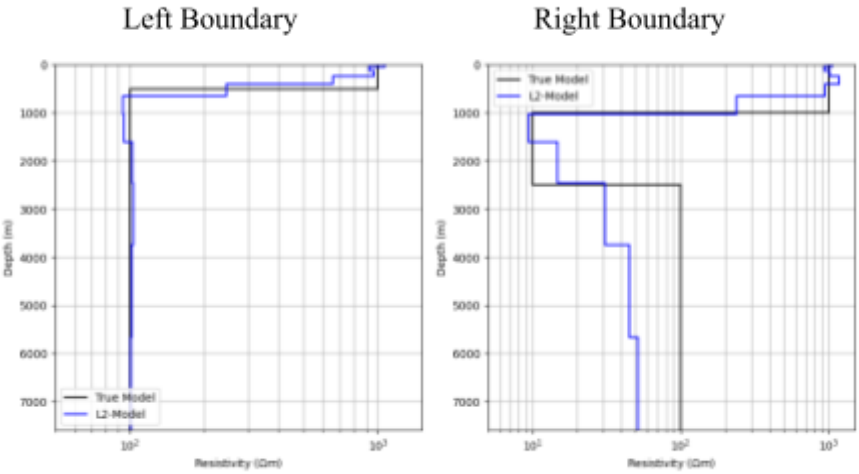

Figure 10: Recovered 1D at the Left and Right Boundaries with GF=1.5

As anticipated, when using a smaller geometric factor, the resulting model “overfits” and exhibits excessive sinusoidal behavior, lacking the distinct sharp-block shape characteristic of the original model.

On the other hand, selecting a larger geometric factor yields a more blocky shape, effectively capturing the simpler model on the left-hand side. However, on the more complex right side, where three layers are present, the model struggles to accurately capture the third layer due to limitations in resolving sharp resistivity contrasts inherent in the reference model with thicker layers.

Through experimentation, it was determined that a geometric factor of approximately 1.2 achieves the most balanced result. This value strikes an optimal compromise between capturing the intricate details of the model while avoiding excessive sinusoidal artifacts.

6.1.2 Tuning BetaEstimate_ByEig Value

Maintaining the geometric factor at 1.2, the beta0_ratio parameter of the BetaEstimate_ByEig method (which indicates the ratio between data misfit and the model objective function at the initial beta iteration) was adjusted across three different orders of magnitude. This adjustment aimed to identify the optimal value for the parameter.

<u>beta0_ratio=1e1:</u>

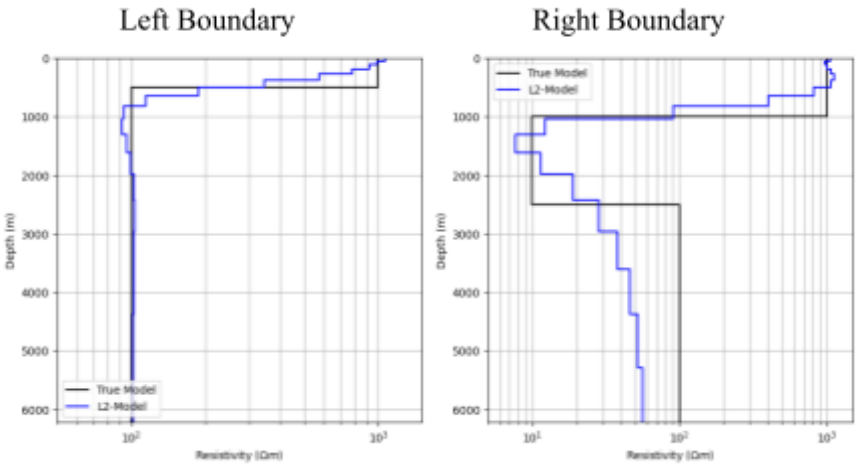

Figure 11: Recovered 1D at the Left and Right Boundaries with beta0_ratio=1e1

beta0_ratio=1e0:

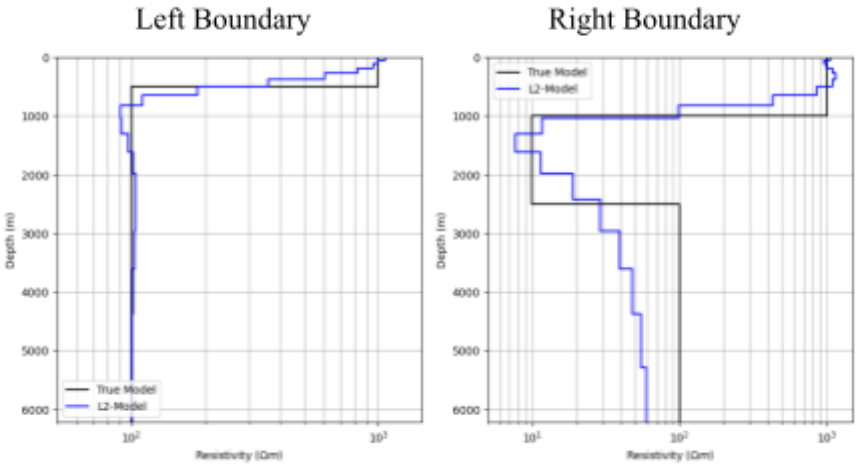

Figure 12: Recovered 1D at the Left and Right Boundaries with beta0_ratio=1e0

beta0_ratio=1e-1:

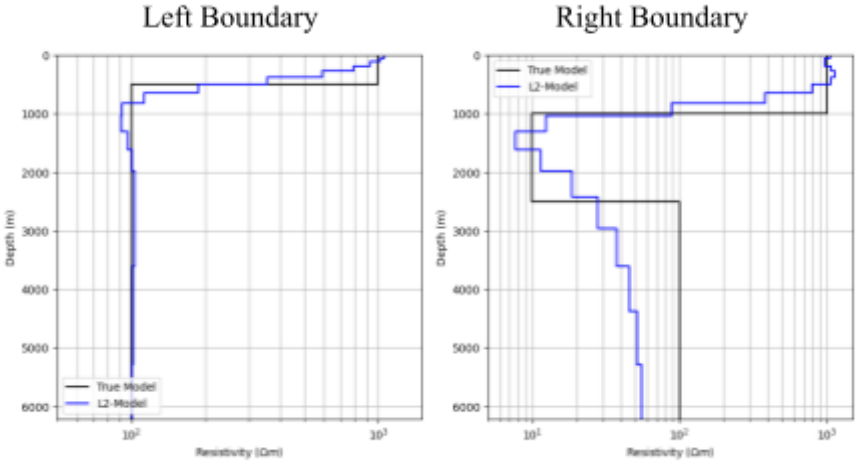

Figure 13: Recovered 1D at the Left and Right Boundaries with beta0_ratio=1e-1

After experimenting with various magnitudes, it was found that a magnitude of 1e0 produced the most satisfactory results. This determination was based on the close agreement observed between the recovered model and the actual model, particularly in deeper depths ranging from 4000m to 5000m.

6.2. Final Result

Finally the inversion process was then applied to each survey location using the parameters selected earlier. The resulting models were projected onto the 2D grid outlined in the "Experimental Setup" section. Below is the raw output obtained from the inversion of the entire region:

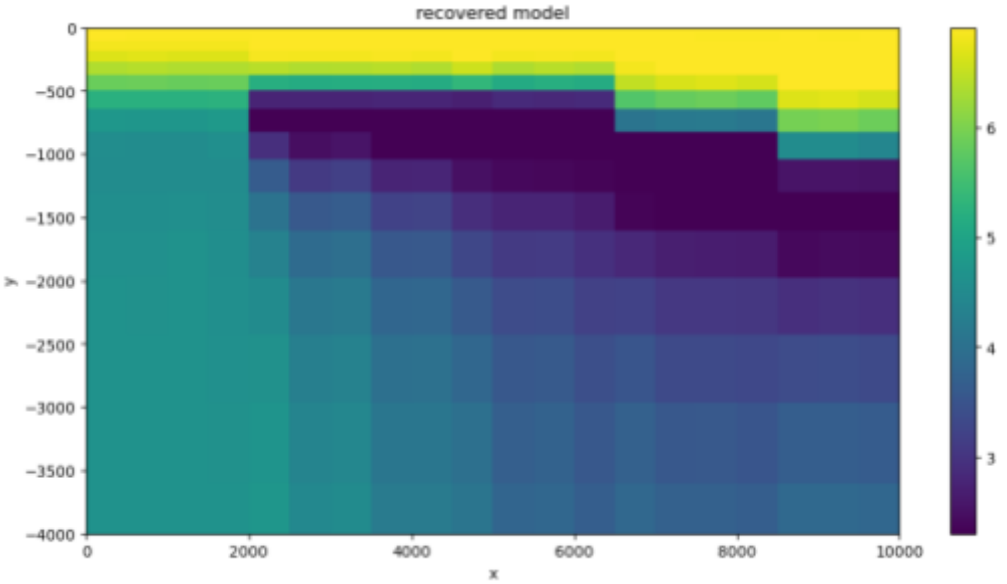

Figure 14: Recovered Model (L2)

Following this, the recovered models were subjected to linear interpolation, incorporating four interpolated points horizontally between each pair of original sounding points. This interpolation process aimed to restore smoothness to the model, as the reference model possessed a smooth boundary that was compromised during discretization.

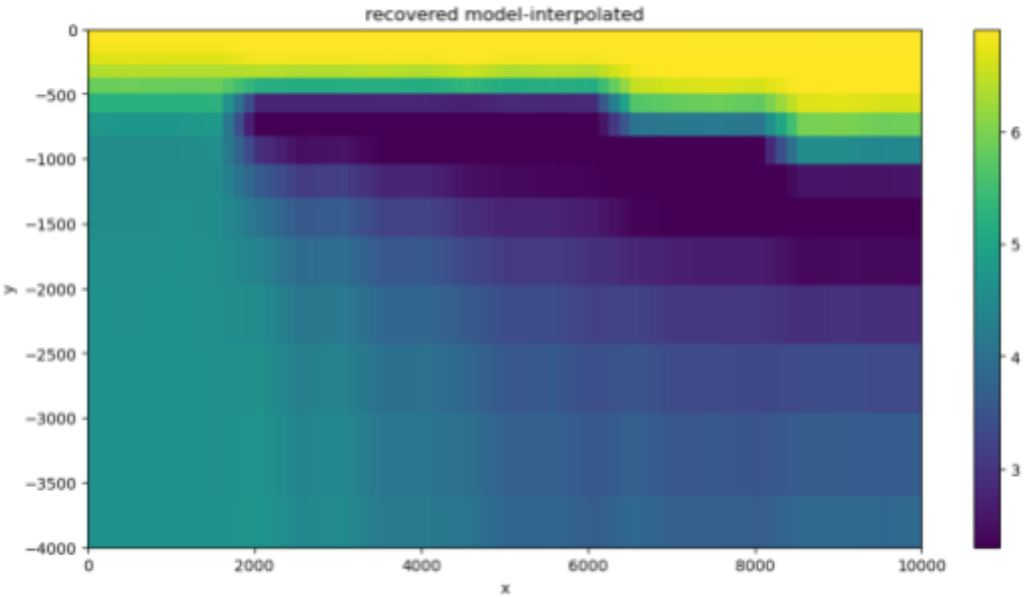

Figure 15: Linearly Interpolated Recovered Model (L2)

As depicted in the above figures, the 2D substructure was successfully reconstructed within the correct region with approximately accurate log resistivity values. However, unlike the reference model, the boundaries between different resistivity layers appear less sharp, displaying a more gradual transition. This observation aligns with the results of inversion tests conducted at the left and right corners, where the resulting model exhibited a "curvy" rather than "blocky" structure. This characteristic is inherent to the least squares inversion technique, which tends to regularize the model, favoring smooth structures that may not precisely reflect the true model. In an effort to recover sparser and/or blockier 1D structures, an alternative method, the iteratively re-weighted least-squares approach, was explored.

7. Inversion Method 2: Iteratively Reweighted Least- Square Method

The second inversion method explored is the Iteratively Reweighted Least-Square Method. This method can yield a more blocky result compared to the first inversion methods due to its ability to promote sparsity in the recovered model. By emphasizing the sparsity-inducing norms, such as the L1 norm, in the regularization term, the IRLS method encourages the solution to have fewer nonzero components, resulting in a blockier model with sharp transitions between different geological features.

The IRLS method penalizes the presence of many small values in the recovered model, favoring solutions with fewer distinct values. This tendency towards sparsity and blockiness makes the IRLS method particularly suitable for recovering models with sparse and blocky structures, such as those encountered in geophysical applications.

The inversion directives for this method include UpdateSensitivityWeights, UpdatePreconditioner, and BetaEstimate_ByEig, as previously described. Notably, the BetaSchedule and TargetMisfit directives are not utilized in this method. Instead, the beta cooling schedule is specified within the Update_IRLS directive, where the coolingFactor and coolingRate properties are adjusted to control the rate of convergence. Additionally, the target misfit for the L2 portion of the IRLS approach is defined using the chifact_start property.

To attain the desired outcome, the values in the directives did not need to be changed, but it was necessary to increase the geometric factor.

7.1. 1D Inversion Results

Following are inversion results of various geometric factors.

GF=1.2 (Optimal for L2 Inversion):

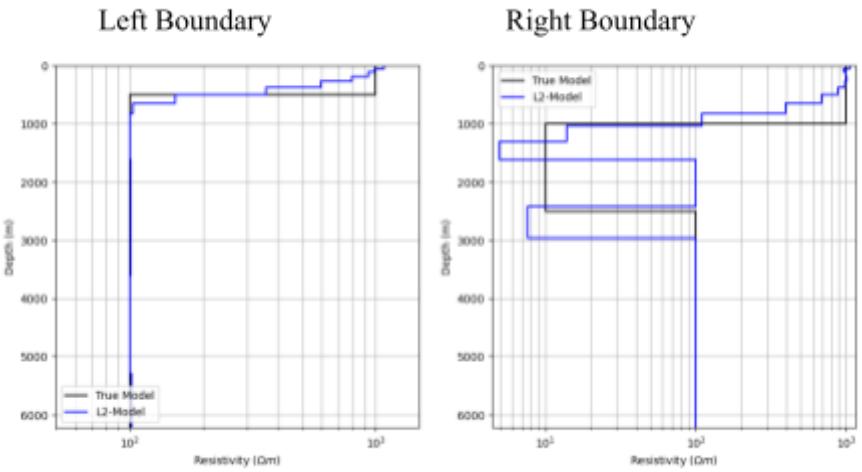

Figure 16: Recovered 1D at the Left and Right Boundaries with GF=1.2

GF=1.5:

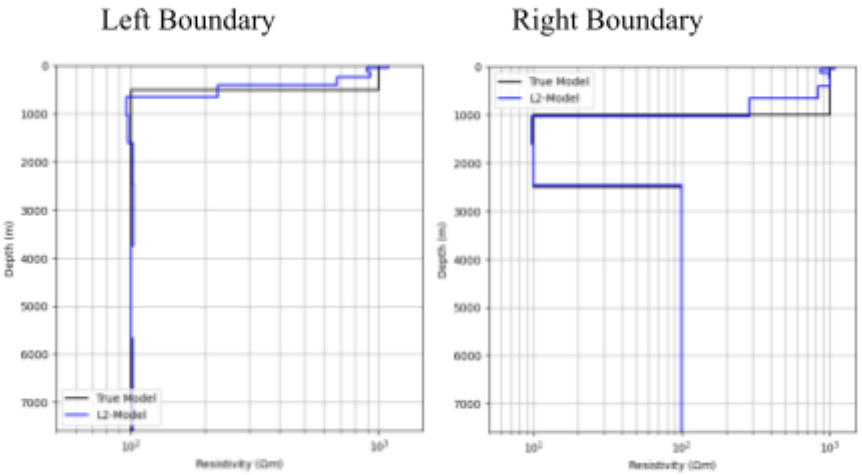

Figure 17: Recovered 1D at the Left and Right Boundaries with GF=1.5

GF=1.8:

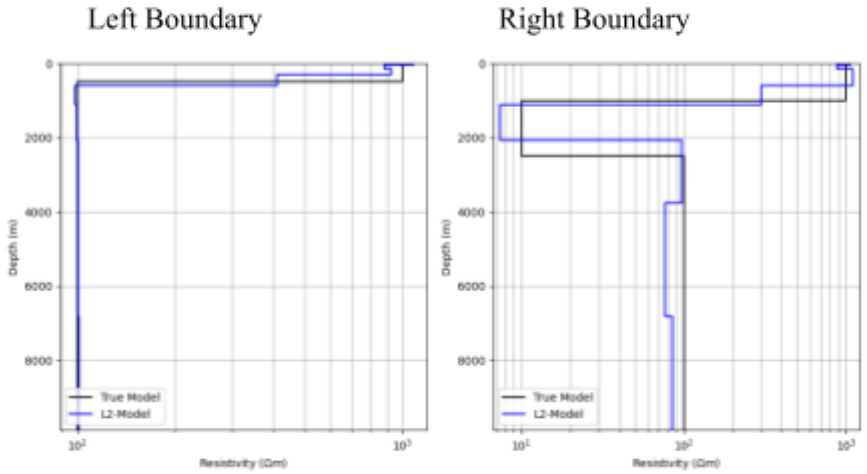

Figure 18: Recovered 1D at the Left and Right Boundaries with GF=1.8

The optimal geometric factor (GF) for this method was determined to be 1.5, significantly higher than the optimal GF for the first inversion method. This difference arises from the nature of the IRLS method, which penalizes the presence of numerous small values in the recovered model. It favors solutions with fewer distinct model parameters, a characteristic achieved by employing a larger GF. However, it's important to note that excessively large GF values can lead to information loss and subsequently degrade the quality of the recovered model, even with this method.

Here is a comparison between the Weighted Least Square method (L2) and the Iteratively Reweighted Least Square method (IRLS):

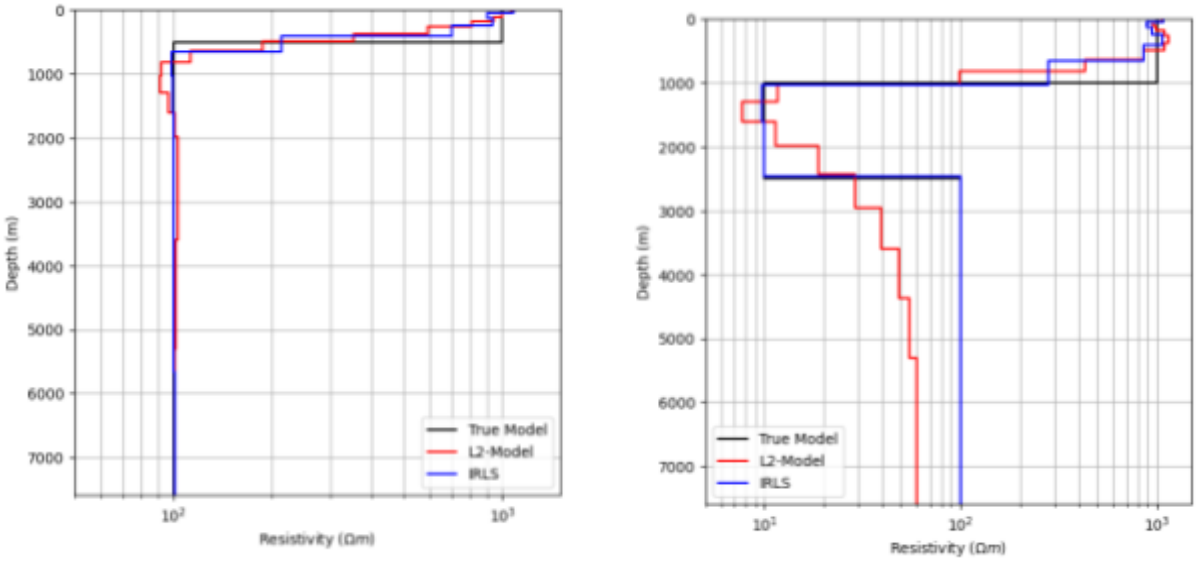

Figure 19: Comparison of Recovered Model with Different Inversion Method

As you can see with the Iteratively Reweighted Least Square method, we can achieve a much desirable, or “blockly”, result.

8.2. Final Result

Following are the raw output obtained from the inversion of the entire region for this method:

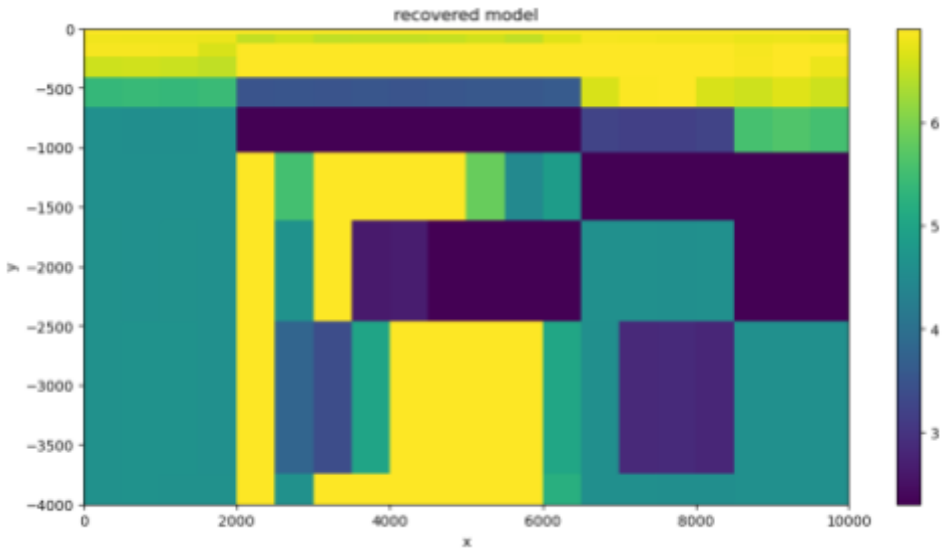

Figure 20: Recovered Model (IRLS)

Following is the linearly interpolated result for this method:

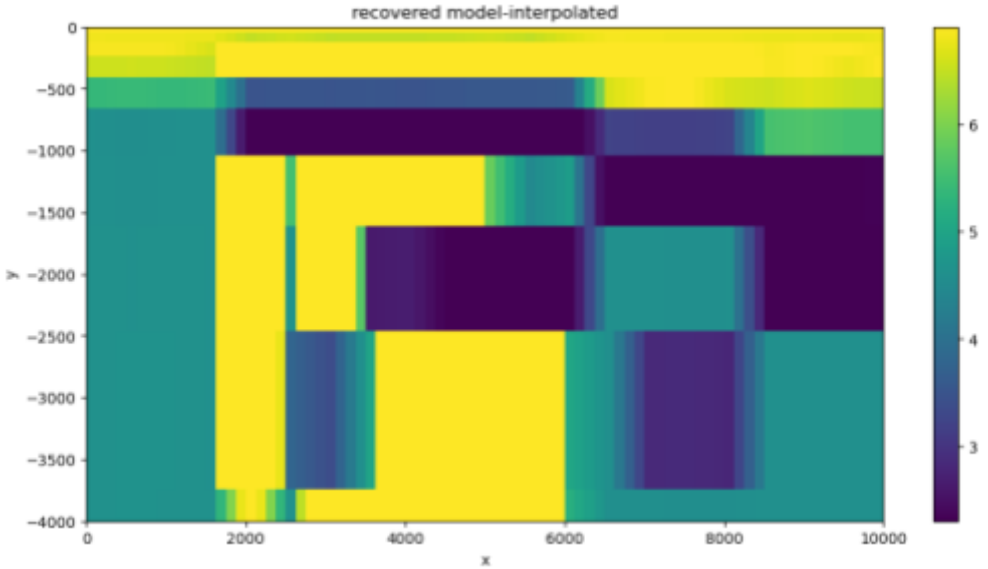

Figure 21: Linearly Interpolated Recovered Model (IRLS)

As observed, while the 1D inversion at the boundaries appeared promising, the final result exhibits significant noise, particularly in the middle section. This noise is primarily attributed to the rigorous penalization inherent in the IRLS method. In contrast to the first method, where the model can abruptly transition from one extreme to another when encountering a small change, the IRLS method imposes a stricter penalty, leading to a recovered model with a high level of noise. This can be seen by examined the recovered model at the x=5000m point:

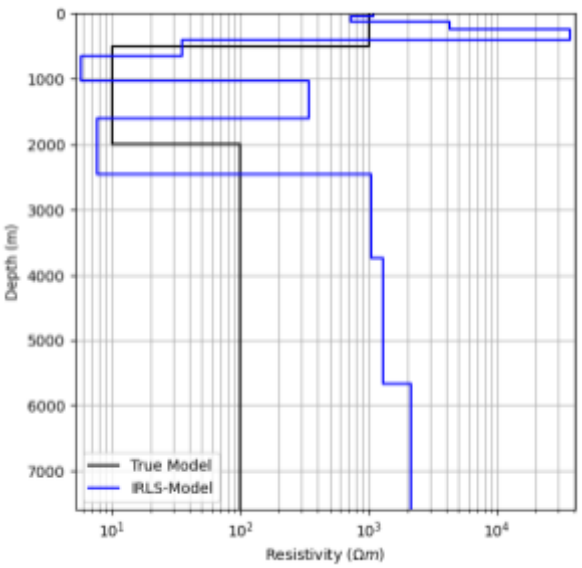

Figure 22: Recovered IRLS Model at x=5000m

To address this issue, adjusting the geometric factor for each sounding could potentially improve the results. However, implementing such a strategy for every individual sounding is impractical in real-world applications. Consequently, this approach is less suitable for the objectives of this project.

9. Conclusion

In this project, we investigated two inversion methods, namely the weighted least squares approach and the Iteratively Reweighted Least Squares method, to characterize 2D subsurface structures using frequency domain electromagnetic data. Through our exploration, we aimed to assess the accuracy of these methods in recovering subsurface features.

The weighted least squares approach exhibited limitations in accurately capturing sharp boundaries between different resistivity layers. Despite its ability to generate smooth models, the method struggled to represent the sharp resistivity contrasts of the subsurface structures.

In contrast, the IRLS method showed potential in recovering blockier models with sharper transitions between resistivity layers. However, its stringent penalization of small values in the recovered model led to increased noise levels, especially in regions with more than two layers of geological features.

Hence for this project, the weighted least squares approach proved to be a better choice, as it recovered a model much closer to the target/reference model.

Overall, this project highlighted the importance of selecting appropriate inversion methods and parameter values based on the specific characteristics of the subsurface structure and the goals of the investigation.

10. References

- De Groot‐Hedlin, C., & Constable, S. (2004). Inversion of magnetotelluric data for 2D structure with sharp resistivity contrasts. Geophysics, 69(1), 78–86. https://doi.org/10.1190/1.1649377
- https://em.geosci.xyz/content/physical_properties/electrical_conductivity/index.html#electrical-conductivity-index
- https://em.geosci.xyz/content/geophysical_surveys/airborne_fdem/data.html